The NEW ENGLAND JOURNAL of MEDICINE

ESTABLISHED IN 1812 JUNE 19, 2003 VOL. 348 NO. 25

# Noninvasive Detection of Clinically Occult Lymph-Node Metastases in Prostate Cancer

Mukesh G. Harisinghani, M.D., Jelle Barentsz, M.D., Ph.D., Peter F. Hahn, M.D., Ph.D., Willem M. Deserno, M.D., Shahin Tabatabaei, M.D., Christine Hulsbergen van de Kaa, M.D., Ph.D., Jean de la Rosette, M.D., Ph.D., and Ralph Weissleder, M.D., Ph.D.

## ABSTRACT

### BACKGROUND

Accurate detection of lymph-node metastases in prostate cancer is an essential component of the approach to treatment. We investigated whether highly lymphotropic superparamagnetic nanoparticles, which gain access to lymph nodes by means of interstitial–lymphatic fluid transport, could be used in conjunction with high-resolution magnetic resonance imaging (MRI) to reveal small nodal metastases.

### METHODS

Eighty patients with presurgical clinical stage T1, T2, or T3 prostate cancer who underwent surgical lymph-node resection or biopsy were enrolled. All patients were examined by MRI before and 24 hours after the intravenous administration of lymphotropic superparamagnetic nanoparticles (2.6 mg of iron per kilogram of body weight). The imaging results were correlated with histopathological findings.

### RESULTS

Of the 334 lymph nodes that underwent resection or biopsy, 63 (18.9 percent) from 33 patients (41 percent) had histopathologically detected metastases. Of these 63 nodes, 45 (71.4 percent) did not fulfill the usual imaging criteria for malignancy. MRI with lymphotropic superparamagnetic nanoparticles correctly identified all patients with nodal metastases, and a node-by-node analysis had a significantly higher sensitivity than conventional MRI (90.5 percent vs. 35.4 percent, $P<0.001$) or nomograms.

### CONCLUSIONS

High-resolution MRI with magnetic nanoparticles allows the detection of small and otherwise undetectable lymph-node metastases in patients with prostate cancer.

From Massachusetts General Hospital and Harvard Medical School, Boston (M.G.H., P.F.H., S.T., R.W.); and University Medical Center, Nijmegen, the Netherlands (J.B., W.M.D., C.H.K., J.R.). Address reprint requests to Dr. Weissleder at the Center for Molecular Imaging Research, Department of Radiology, Massachusetts General Hospital, Bldg. 149, 13th St., Rm. 5403, Charlestown, MA 02129-2060, or at weissleder@helix.mgh.harvard.edu.

Drs. Harisinghani and Barentsz contributed equally to the article.

N Engl J Med 2003;348:2491-9.

In 2001, about 198,000 new cases of prostate cancer were diagnosed in the United States and 31,500 men died of the disease.[1] The natural history and aggressiveness of the disease vary widely, and the means to identify men with clinically occult lymph-node metastases is greatly needed.[2-8] The adverse prognostic implications of lymph-node metastases have been widely established.[9,10]

Magnetic resonance imaging (MRI) provides images with excellent anatomical detail and soft-tissue contrast but is relatively insensitive for the detection of lymph-node metastases.[11] However, the results of MRI can be improved by using different imaging agents and acquisition techniques.[12-14] In particular, the use of lymphotropic superparamagnetic nanoparticles holds considerable promise.[15-18] As shown in Figure 1, these nanoparticles have a monocrystalline, inverse spinel, superparamagnetic iron oxide core, contain a dense packing of dextrans to prolong their time in circulation, and are avidly taken up by lymph nodes in animals[16] and humans.[19] The nanoparticles are slowly extravasated from the vascular into the interstitial space, from which they are transported to lymph nodes by way of lymphatic vessels (Fig. 1).[16] Within the lymph nodes, lymphotropic superparamagnetic nanoparticles are internalized by macrophages, and these intracellular iron-containing particles cause changes in magnetic properties detectable by MRI.[20]

We investigated whether lymphotropic superparamagnetic nanoparticles can be used in conjunction with MRI to detect metastatic tumor in local and distant lymph nodes in humans, as they have been used in mouse models.[20] We were particularly interested in cases in which metastases had not caused an increase in the size of the lymph node (clinically occult disease). We prospectively determined the accuracy of the method in 334 lymph nodes in 80 patients with biopsy-proven prostate cancer who subsequently underwent resection of the tumor or pelvic lymph nodes (or both) or a targeted lymph-node biopsy.

## METHODS

### PATIENTS

Patients with a resectable prostate cancer as determined by conventional imaging methods, digital rectal examination, an ultrasound-guided sextant core biopsy, and measurement of serum prostate-specific antigen levels were enrolled in this study according to established surgical practice.[21,22] All patients had stage T1, T2, or T3 prostate cancer before surgical intervention. The first cohort consisted of 40 patients who were treated at Massachusetts General Hospital in Boston between 1999 and 2002. The second cohort consisted of 40 patients who were treated at the University Medical Center in Nijmegen, the Netherlands, between 1999 and 2001. All 80 men gave informed written consent and completed the study. The studies were approved by the medical ethics committees of the respective hospitals.

### LYMPHOTROPIC SUPERPARAMAGNETIC NANOPARTICLES

The lymphotropic superparamagnetic nanoparticle used in this study was a monocrystalline iron oxide (Combidex, Advanced Magnetics, in the United States and Sinerem, Guerbet, in the Netherlands; Combidex and Sinerem are identical).[23] The lyophilized iron oxide was reconstituted in normal saline and injected at a dose of 2.6 mg of iron per kilogram of body weight over a period of 15 to 30 minutes. Five patients reported low back pain during the infusion, which disappeared after the infusion was temporarily stopped; the pain did not recur when the infusion was resumed. All patients received the full dose and completed the entire study.

### MAGNETIC RESONANCE IMAGING

MRI was performed at 1.5 T with the use of state-of-the-art imaging systems (Magnetom Vision, Siemens, in the 40 patients in the Netherlands and Horizon, GE Medical Systems, in the 40 patients in the United States) and pelvic phased-array coils. Images of the pelvis, extending from the pubic symphysis to the level of aortic bifurcation, were obtained before and 24 hours after the intravenous administration of lymphotropic superparamagnetic nanoparticles. Details of the pulse sequences are given in Supplementary Appendix 1 (available with the full text of this article at http://www.nejm.org). The images were evaluated at workstations in a blinded fashion by two experienced readers and analyzed as described below.

### IMAGE ANALYSIS

On conventional MRI, lymph nodes were classified as malignant if the short-axis diameter was elongated and exceeded 10 mm or was rounded and exceeded 8 mm, according to standard criteria.[24] On MRI

with lymphotropic superparamagnetic nanoparticles, nodes were considered malignant when one of the following three criteria were present: a decrease in signal intensity of less than 30 percent on $T_2$-weighted fast spin–echo or gradient-echo sequences after the administration of lymphotropic superparamagnetic nanoparticles; a heterogeneous signal (giving the entire node a mottled appearance), discrete focal defects (isolated islands of high signal intensity), or both; and nodes with a central area of hyperintensity (excluding a fatty hilum) but a peripheral decrease in signal intensity. The signal-to-noise ratios of lymph nodes were determined by manually marking regions of interest over lymph nodes on different scans and pulse sequences. A receiver-operating-characteristic (ROC) curve analysis was also performed by two readers who were unaware of the patients' serum prostate-specific antigen level, clinical stage, or Gleason score. The diagnostic standard was histopathological evaluation of each lymph node. Three-dimensional reconstructions of the pelvic anatomy were also obtained (Advantage Windows version 3.1, GE Medical Systems) in a subgroup of 40 patients to aid in the approach to surgery and radiotherapy.

## SURGERY

Open resections were performed in 60 patients, and 15 patients underwent a laparoscopic resection. In five patients, the presence or absence of nodal metastases in specific lymph nodes was ascertained by computed-tomography–guided biopsy and no surgery was performed. Open and laparoscopic dissection of pelvic lymph nodes consisted of a generally accepted resection of left and right obturator lymph nodes and included more extensive exploration in nine patients because of suggestive findings on imaging. To ensure optimal correlation, the surgeon was given a schematic drawing or a three-dimensional rendering identifying all the lymph

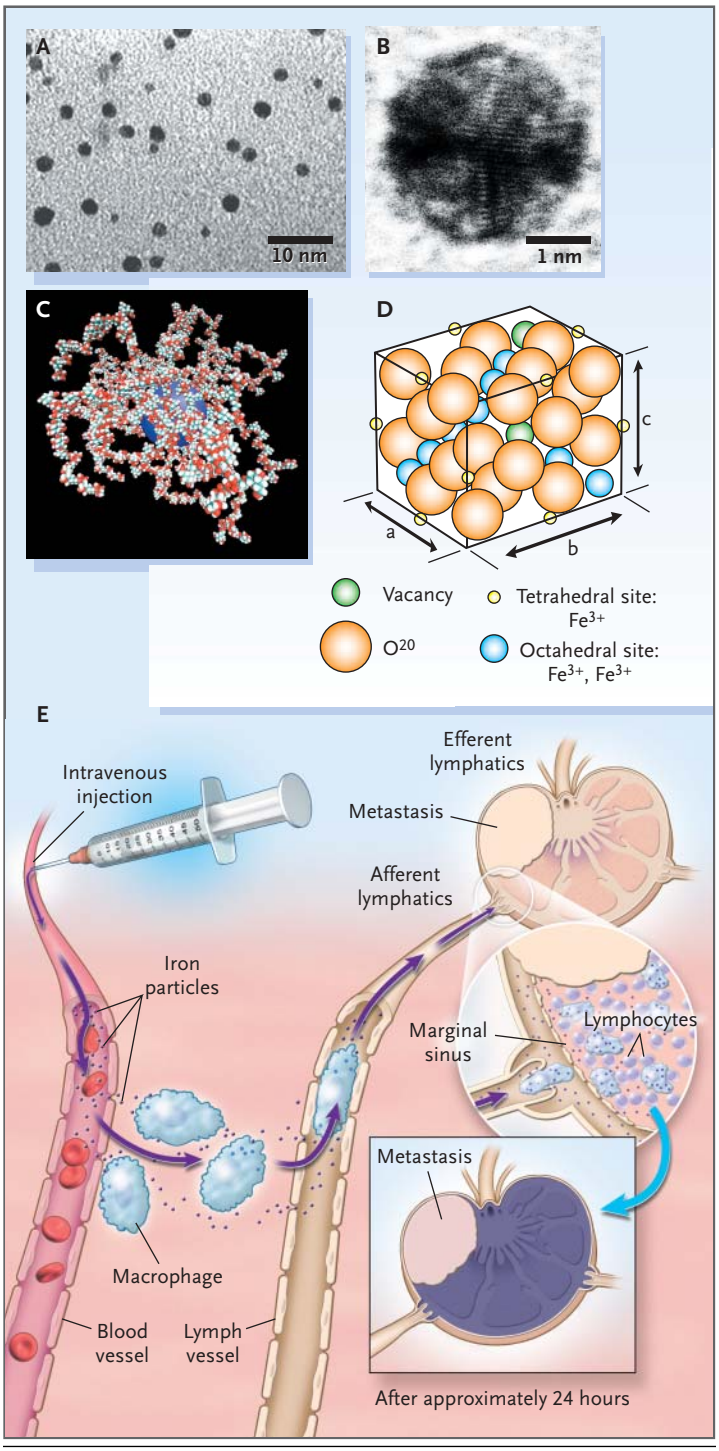


**Figure 1. Electron Micrograph of Hexagonal Lymphotropic Superparamagnetic Nanoparticles (Panels A and B), Molecular Model of Surface-Bound 10-kD Dextrans and Packing of Iron Oxide Crystals (Panels C and D), and Mechanism of Action of Lymphotropic Superparamagnetic Nanoparticles (Panel E).**

The model lymphotropic superparamagnetic nanoparticles shown here measure 2 to 3 nm on average (Panels A and B). The mean overall particle size of the 10-kD dextrans is 28 nm (Panels C and D). In Panel E, the systemically injected long-circulating particles gain access to the interstitium and are drained through lymphatic vessels. Disturbances in lymph flow or in nodal architecture caused by metastases lead to abnormal patterns of accumulation of lymphotropic superparamagnetic nanoparticles, which are detectable by MRI.

nodes in relation to the iliac vessels. Resected nodes were placed on a grid identifying their location and orientation and then sent for histopathological analysis. Multiple sections of all of the resected lymph nodes were stained with hematoxylin and eosin, and the slides were reviewed by at least two pathologists who had no knowledge of the MRI findings. The histopathological results for each lymph node were catalogued for subsequent comparison with MRI findings.

### STATISTICAL ANALYSIS

The statistical significance of the sensitivities and specificities of conventional MRI and MRI with lymphotropic superparamagnetic nanoparticles was calculated with the use of McNemar's test, and a two-tailed P value of less than 0.001 was considered to indicate statistical significance. For comparison among the groups, Fisher's exact test was used, with a P value of less than 0.001 considered to indicate statistical significance. Accuracy was defined as the percentage of all patients or lymph nodes in which MRI with lymphotropic superparamagnetic nanoparticles correctly predicted the presence or absence of metastatic tumor, calculated with the following equation: (true positive + true negative) ÷ (true positive + true negative + false positive + false negative).

For the ROC analysis, the readers were asked to assign one of five confidence levels to each node. The readers had no knowledge of the correct histopathological diagnosis. A binomial ROC curve was fitted to the confidence rating assigned by each observer with a maximum likelihood estimation.[25] The diagnostic accuracy of MRI studies before and after the administration of lymphotropic superparamagnetic nanoparticles as determined by each observer was evaluated by calculating the area under the ROC curve. Interobserver agreement with respect to the evaluation of both MRI studies was assessed with use of the kappa statistic.[26]

The likelihood of lymph-node metastases on the basis of a nomogram was calculated with the use of established criteria: low risk was defined by an incidence of nodal metastases of less than 4 percent if the serum prostate-specific antigen level was less than 10 ng per milliliter, the Gleason score was less than 6, and stage T1 prostate cancer was present; intermediate risk was defined by 18 percent incidence of nodal metastases if the serum prostate-specific antigen level was 10 to 20 ng per milliliter, the Gleason score was 6 or 7, and stage T1 prostate cancer was present; and high risk was defined by a very high but variable incidence of nodal metastases if the serum prostate-specific antigen level exceeded 20 ng per milliliter, the Gleason score exceeded 7, and stage T2 or greater prostate cancer was present.[27,28] Statistical analysis was carried out with the use of SAS software.

## RESULTS

### CHARACTERISTICS OF THE PATIENTS

A total of 80 patients with pathologically proven prostate cancer were enrolled in the study (Table 1), and a total of 334 lymph nodes with direct MRI–histologic correlations were evaluated. Of the 334 lymph nodes, 271 were benign (81.1 percent) and 63 lymph nodes (18.9 percent) — from 33 patients (41 percent) — contained microscopically detectable metastases. Of these 63 nodes, 17 measured less than 5 mm, 28 were 5 to 10 mm, and 18 exceeded 10 mm. Overall, 71.4 percent of the malignant nodes did not fulfill the traditional imaging criteria for malignancy (more than 10 mm if elongated or more than 8 mm if rounded).

### DIAGNOSIS

Figure 2 shows representative examples of retroperitoneal images from three patients. In normal lymph nodes, the signal intensity decreased homogeneously after the administration of lymphotropic superparamagnetic nanoparticles, indicating normal delivery of the nanoparticles to the lymph nodes and normal uptake of the particles by nodal macrophages. In lymph nodes containing metastases, there was either a limited decrease in signal intensity or discrete focal defects within the node owing to replacement of nodal architecture by tumor deposits. In the representative example shown in Figures 2G, 2H, and 2I, MRI with lymphotropic superparamagnetic nanoparticles facilitated the detection of 2-mm metastases in retroperitoneal nodes. Figure 3A shows a three-dimensional rendering of normal (green) and metastatic (red) lymph nodes superimposed onto vascular maps derived from the same imaging sequence. In this rendering, the relation of individual nodes to vascular landmarks can be established. This example also illustrates how readily malignant iliac nodes can be distinguished from adjacent benign nodes on MRI after the administration of lymphotropic superparamagnetic nanoparticles (Fig. 3C) but not before (Fig. 3B).

### SENSITIVITY

Table 2 summarizes the quantitative analysis of all patients on the basis of objective changes in the sig-

**Table 1. Characteristics of the 80 Patients in the Study.**

| Characteristic | Value |
|---|---|
| Age (yr) | |
| Mean | 64 |
| Range | 54–75 |
| Serum prostate-specific antigen (ng/ml) | |
| Median | 21 |
| Range | 4–80 |
| Gleason score* | |
| Mean | 7 |
| Range | 5–8 |
| Nomogram for predicting nodal metastases (% of patients)† | |
| Low risk | 15 |
| Intermediate risk | 60 |
| High risk | 25 |
| Lymph nodes (total no.) | |
| No. examined | 334 |
| Short-axis diameter <5 mm | 125 |
| Short axis diameter 5–10 mm | 185 |
| Short-axis diameter >10 mm | 24 |
| Positive nodes | 63 |
| Negative nodes | 271 |
| Lymph-node metastases | |
| Short-axis diameter <5 mm (total no.) | 17 |
| Short-axis diameter 5–10 mm (total no.) | 28 |
| Short-axis diameter 8–10 mm and rounded (total no.) | 20 |
| Short-axis diameter >10 mm (total no.) | 18 |
| Incidence of nodal metastases on a node-by-node basis (%) | 18.9 |
| Nodal metastases (% of patients) | 41 |

* The Gleason score can range from 2 to 10, with higher scores indicating more aggressive disease.

† Low risk was defined by an incidence of nodal metastases of less than 4 percent if the serum prostate-specific antigen level was less than 10 ng per milliliter, the Gleason score was less than 6, and stage T1 prostate cancer was present; intermediate risk was defined by an 18 percent incidence of nodal metastases if the serum prostate-specific antigen level was 10 to 20 ng per milliliter, the Gleason score was 6 or 7, and stage T1 prostate cancer was present; and high risk was defined by a very high but variable incidence of nodal metastases if the serum prostate-specific antigen level exceeded 20 ng per milliliter, the Gleason score exceeded 7, and stage T2 or greater prostate cancer was present.[27,28]

nal intensity of MRI. On MRI with lymphotropic superparamagnetic nanoparticles, the signal-to-noise ratios of normal nodes decreased from a mean (±SD) of 192±24 to 69.7±16 on $T_2$-weighted sequences, and the decrease was homogeneous across lymph nodes. Objective signs such as a limited decrease in signal intensity (P<0.001), the presence of hyperintense foci within nodes (P<0.001), or a mottled appearance on gradient-echo images (P<0.001) were all highly specific for nodal metastases. On a patient-by-patient analysis (Table 2), MRI with lymphotropic superparamagnetic nanoparticles correctly identified all patients with metastases (100 percent sensitivity). Among patients free of lymph-node metastases, MRI with lymphotropic superparamagnetic nanoparticles provided the correct diagnosis in 96 percent. MRI with lymphotropic superparamagnetic nanoparticles was also more accurate than conventional MRI with respect to published and validated nomograms for predicting lymph-node metastases.[27,28] In the low-risk group of 12 patients, 1 had nodal metastases (true incidence, 8 percent; estimated risk, less than 4 percent). In the intermediate-risk group, 15 of 48 patients had nodal metastases (true incidence, 31 percent; estimated risk, 18 percent), and in the high-risk group, 17 of 20 patients had metastases (true incidence, 85 percent).

On a node-by-node basis, the overall sensitivity of MRI with lymphotropic superparamagnetic nanoparticles was 90.5 percent and was significantly higher (P<0.001) than that of conventional MRI (sensitivity, 35.4 percent). Similarly, the administration of lymphotropic superparamagnetic nanoparticles improved the diagnostic specificity from 90.4 percent to 97.8 percent. For lymph nodes with a diameter of 5 to 10 mm on the short axis, which would be considered normal on conventional MRI, the sensitivity of MRI with lymphotropic superparamagnetic nanoparticles was 96.4 percent. In all nine of the patients in whom the latter method suggested the presence of metastases in lymph nodes not classically considered to be candidates for resection and who underwent more extensive exploration, metastases were histologically confirmed at distant sites. The false positive nodes were all larger than 10 mm and showed reactive hyperplasia on staining, which most likely resulted in heterogeneous uptake of lymphotropic superparamagnetic nanoparticles. All false negative nodes had a short-axis diameter of less than 5 mm, which is probably below the current detection threshold of MRI. ROC analysis indicated that the areas under the curve were significantly higher for MRI with lymphotropic superparamagnetic nanoparticles than for conventional MRI (0.975 vs. 0.756, P<0.001).

## DISCUSSION

A sensitive and reliable means of detecting lymph-node metastases in men with prostate cancer is im-

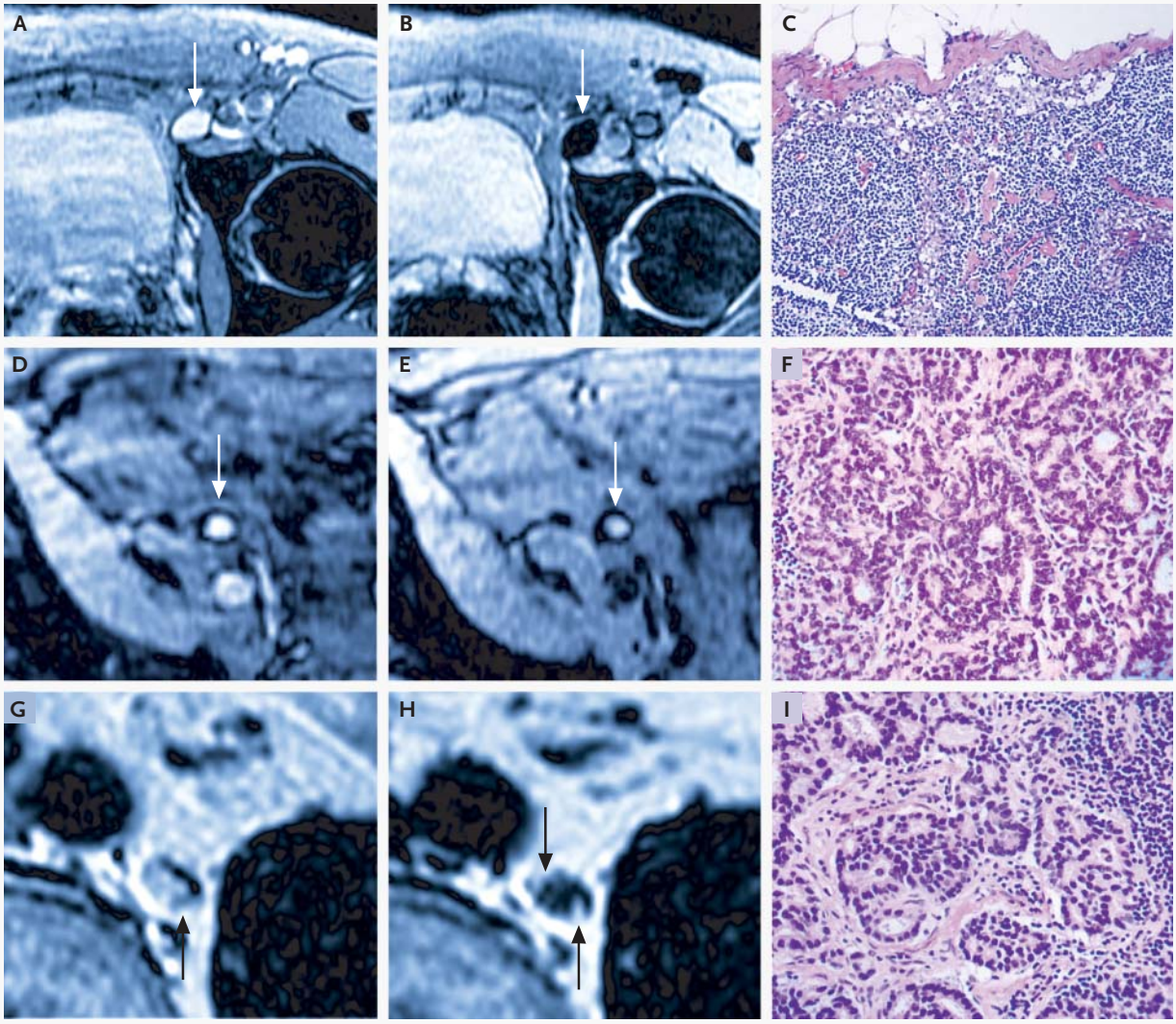


**Figure 2. MRI Nodal Abnormalities in Three Patients with Prostate Cancer.**

As compared with conventional MRI (Panel A), MRI obtained 24 hours after the administration of lymphotropic superparamagnetic nanoparticles (Panel B) shows a homogeneous decrease in signal intensity due to the accumulation of lymphotropic superparamagnetic nanoparticles in a normal lymph node in the left iliac region (arrow). Panel C shows the corresponding histologic findings (hematoxylin and eosin, ×125). Conventional MRI shows a high signal intensity in an unenlarged iliac lymph node completely replaced by tumor (arrow in Panel D). Nodal signal intensity remains high (arrow in Panel E). Panel F shows the corresponding histologic findings (hematoxylin and eosin, ×200). Conventional MRI shows high signal intensity in a retroperitoneal node with micrometastases (arrow in Panel G). MRI with lymphotropic superparamagnetic nanoparticles demonstrates two hyperintense foci (arrows in Panel H) within the node, corresponding to 2-mm metastases. Corresponding histologic analysis confirms the presence of adenocarcinoma within the node (Panel I, hematoxylin and eosin, ×200).

portant because patients with truly local disease have the options of radical prostatectomy, watchful waiting, and radiotherapy.[2,5] In men with locally advanced or metastatic disease, however, adjuvant androgen-deprivation therapy with radiation is the mainstay of management.[3,4,29]

We found that lymph-node metastases can be accurately diagnosed by high-resolution MRI with lymphotropic superparamagnetic nanoparticles but not by conventional MRI. On a patient-by-patient basis, the addition of lymphotropic superparamagnetic nanoparticles increased the sensitivity of MRI

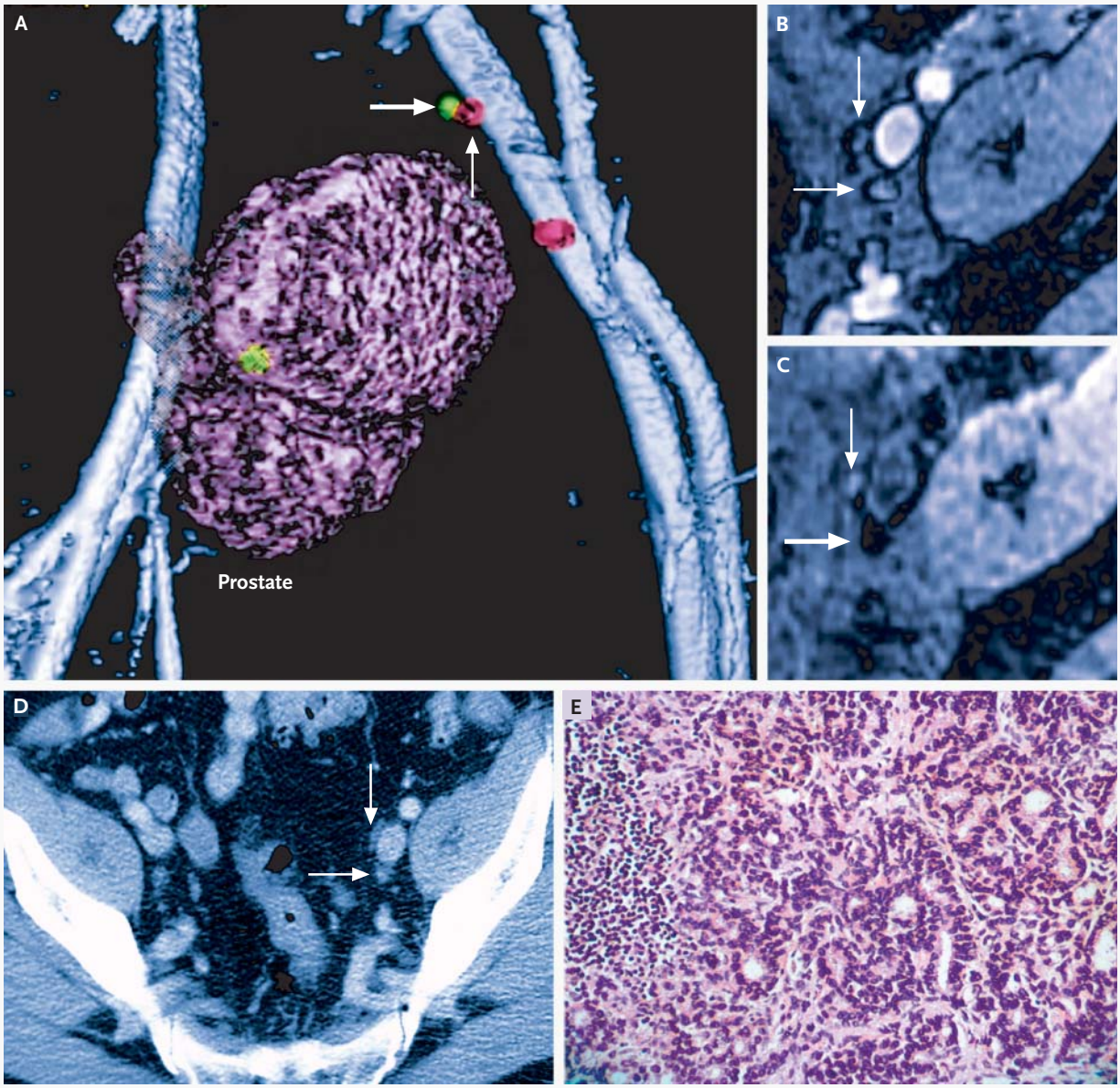


**Figure 3. Three-Dimensional Reconstruction of Pelvic Lymph Nodes (Panel A), Conventional MRI (Panel B), MRI with Lymphotropic Superparamagnetic Nanoparticles (Panel C), Abdominal Computed Tomography (CT) (Panel D), and Histopathological Findings (Panel E).**

Panel A shows a three-dimensional reconstruction of the prostate, iliac vessels, and metastatic (red) and nonmetastatic (green) lymph nodes, to assist in the planning of surgery and radiotherapy. There is a malignant node (thick arrow) immediately adjacent to the normal node (thin arrow) posteromedial to the iliac vessels. In Panel B, conventional MRI shows that the signal intensity is identical in the two nodes (arrows). In Panel C, MRI with lymphotropic superparamagnetic nanoparticles shows that the signal in the normal node is decreased (thick arrow) but that it is high in the metastatic node (thin arrow). In Panel D, abdominal CT fails to differentiate between the two lymph nodes (arrows). In Panel E, histopathological examination of the malignant lymph node reveals sheaths of carcinoma cells (hematoxylin and eosin, ×200).

**Table 2. Sensitivity, Specificity, Accuracy, and Positive and Negative Predictive Values of MRI Alone and MRI with Lymphotropic Superparamagnetic Nanoparticles.**

| Variable | MRI Alone | MRI with Lymphotropic Superparamagnetic Nanoparticles | P Value |
|---|---|---|---|
| Results per patient (n=80) | | | |
| Sensitivity (%) | 45.4 | 100 | <0.001 |
| Specificity (%) | 78.7 | 95.7 | |
| Accuracy (%) | 65.0 | 97.5 | |
| Positive predictive value (%) | 60.0 | 94.2 | |
| Negative predictive value (%) | 67.2 | 100 | |
| Results per individual lymph nodes of all sizes (n=334) | | | |
| Sensitivity (%) | 35.4 | 90.5 | <0.001 |
| Specificity (%) | 90.4 | 97.8 | |
| Accuracy (%) | 76.3 | 97.3 | |
| Positive predictive value (%) | 55.9 | 95.0 | |
| Negative predictive value (%) | 80.3 | 97.8 | |
| Area under the curve | 0.756 | 0.975 | <0.001 |
| Results for nodes with a short-axis diameter of 5–10 mm (n=45) | | | |
| Sensitivity (%) | 28.5 | 96.4 | <0.001 |
| Specificity (%) | 87.2 | 99.3 | |
| Accuracy (%) | 78.3 | 98.9 | |
| Positive predictive value (%) | 28.5 | 96.4 | |
| Negative predictive value (%) | 87.2 | 99.3 | |
| Results for nodes with a short-axis diameter of <5 mm (n=17) | | | |
| Sensitivity (%) | 0 | 41.1 | |
| Specificity (%) | 100 | 98.1 | |
| Accuracy (%) | 86.4 | 90.4 | |
| Positive predictive value (%) | NA* | 77.7 | |
| Negative predictive value (%) | 86.4 | 91.3 | |

* NA denotes not applicable.

from 45.4 percent to 100 percent, with a specificity of 95.7 percent. These results confirm earlier work in animal models[20] and preliminary observations in patients with other types of cancer.[19,30-33] Unexpectedly, even very small metastases — less than 2 mm in diameter — were occasionally identified within normal-sized lymph nodes. Such microscopic tumor deposits are below the threshold of detection of any other imaging technique. For comparison, the limit of detection of tumor deposits in the pelvis on positron-emission tomography is often 6 to 10 mm.[34]

Dissection of pelvic lymph nodes is the diagnostic standard for detecting metastatic prostate cancer in iliac lymph nodes and is therefore performed with either an open or a laparoscopic technique in most patients deemed candidates for surgery. This approach, however, has several limitations. First, the area of surgical exploration is limited to groups within the external iliac obturator nodes, but so-called skip metastases to the internal and common iliac nodes are not uncommon and go undetected with the use of this method. Nine examples of this phenomenon were encountered in the 80 patients we studied. Second, the rates of morbidity and complications of 4 to 5 percent with this invasive technique are not negligible. Third, dissection of pelvic lymph nodes is expensive and requires hospitalization. On average, the cost per metastasis diagnosed in patients with a low risk of postsurgical complications is approximately $43,600. Fourth, it is typically a one-time procedure performed at the beginning of cancer treatment.[35] Although these aspects of cost and outcome of MRI with lymphotropic superparamagnetic nanoparticles will have to be studied in larger, prospective clinical trials, this approach could provide clinical and cost benefits.

The routine imaging protocols used in this study are readily available at most MRI centers. We found that the adapted three-dimensional reconstruction techniques were of particular help in displaying and analyzing the massive amount of high-resolution

data. With them, it is feasible to show both normal and abnormal lymph nodes and their location with respect to important surgical landmarks such as vessels, obturator nerves, and ureters in three dimensions.

Supported in part by departmental funds from both institutions to defray imaging costs and by a grant from the National Cancer Institute (RO1CA59649, to Dr. Weissleder). The experimental imaging agent was supplied to the investigators at no cost.

We are indebted to Alex F. Althausen, M.D., W. Scott McDougal, M.D., Francis J. McGovern, M.D., Donald S. Kaufman, M.D., Douglas M. Dahl, M.D., Chin Lee Wu, M.D., Mansi A. Saksena, M.D., James J. Perumpillichira, M.D., Katharina Marten, M.D., James H. Thrall, M.D., Jack Wittenberg, M.D., and Peter R. Mueller, M.D. (all at Massachusetts General Hospital), and R.J.F. Laheij, Ph.D. (University Medical Center, Nijmegen), for facilitating the performance of the trial; to Elkan F. Halpern, Ph.D. (Massachusetts General Hospital), for help with the statistical analysis; and to Scott Gazelle, M.D., Ph.D., and Lee Josephson, Ph.D. (both at Massachusetts General Hospital), for many helpful discussions.

## REFERENCES

1. Greenlee RT, Hill-Harmon MB, Murray T, Thun M. Cancer statistics, 2001. CA Cancer J Clin 2001;51:15-36. [Erratum, CA Cancer J Clin 2001;51:144.]
2. Walsh PC. Surgery and the reduction of mortality from prostate cancer. N Engl J Med 2002;347:839-40.
3. Smith MR, McGovern FJ, Zietman AL, et al. Pamidronate to prevent bone loss during androgen-deprivation therapy for prostate cancer. N Engl J Med 2001;345:948-55.
4. Messing EM, Manola J, Sarosdy M, Wilding G, Crawford ED, Trump D. Immediate hormonal therapy compared with observation after radical prostatectomy and pelvic lymphadenectomy in men with node-positive prostate cancer. N Engl J Med 1999;341:1781-8.
5. Holmberg L, Bill-Axelson A, Helgesen F, et al. A randomized trial comparing radical prostatectomy with watchful waiting in early prostate cancer. N Engl J Med 2002;347:781-9.
6. Eisenberger MA, Blumenstein BA, Crawford ED, et al. Bilateral orchiectomy with or without flutamide for metastatic prostate cancer. N Engl J Med 1998;339:1036-42.
7. D'Amico AV, Cormack RA, Tempany CM. MRI-guided diagnosis and treatment of prostate cancer. N Engl J Med 2001;344:776-7.
8. Brinkmann AO, Trapman J. Prostate cancer schemes for androgen escape. Nat Med 2000;6:628-9.
9. Cheng L, Bergstralh EJ, Cheville JC, et al. Cancer volume of lymph node metastasis predicts progression in prostate cancer. Am J Surg Pathol 1998;22:1491-500.
10. Kothari PS, Scardino PT, Ohori M, Kattan MW, Wheeler TM. Incidence, location, and significance of periprostatic and periseminal vesicle lymph nodes in prostate cancer. Am J Surg Pathol 2001;25:1429-32.
11. Tempany CM, McNeil BJ. Advances in biomedical imaging. JAMA 2001;285:562-7.
12. Kurhanewicz J, Vigneron DB, Males RG, Swanson MG, Yu KK, Hricak H. The prostate: MR imaging and spectroscopy: present and future. Radiol Clin North Am 2000;38:115-38.
13. Hricak H, Dooms GC, Jeffrey RB, et al. Prostatic carcinoma: staging by clinical assessment, CT, and MR imaging. Radiology 1987;162:331-6.
14. Katz-Brull R, Lavin PT, Lenkinski RE. Clinical utility of proton magnetic resonance spectroscopy in characterizing breast lesions. J Natl Cancer Inst 2002;94:1197-203.
15. Weissleder R, Moore A, Mahmood U, et al. In vivo magnetic resonance imaging of transgene expression. Nat Med 2000;6:351-5.
16. Weissleder R, Elizondo G, Wittenberg J, Lee AS, Josephson L, Brady TJ. Ultrasmall superparamagnetic iron oxide: an intravenous contrast agent for assessing lymph nodes with MR imaging. Radiology 1990;175:494-8.
17. Lewin M, Carlesso N, Tung CH, et al. Tat peptide-derivatized magnetic nanoparticles allow in vivo tracking and recovery of progenitor cells. Nat Biotechnol 2000;18:410-4.
18. Perez JM, Josephson L, O'Loughlin T, Hogemann D, Weissleder R. Magnetic relaxation switches capable of sensing molecular interactions. Nat Biotechnol 2002;20:816-20.
19. Harisinghani MG, Saini S, Weissleder R, et al. MR lymphangiography using ultrasmall superparamagnetic iron oxide in patients with primary abdominal and pelvic malignancies: radiographic-pathologic correlation. AJR Am J Roentgenol 1999;172:1347-51.
20. Wunderbaldinger P, Josephson L, Bremer C, Moore A, Weissleder R. Detection of lymph node metastases by contrast-enhanced MRI in an experimental model. Magn Reson Med 2002;47:292-7.
21. Link RE, Morton RA. Indications for pelvic lymphadenectomy in prostate cancer. Urol Clin North Am 2001;28:491-8.
22. Begg CB, Riedel ER, Bach PB, et al. Variations in morbidity after radical prostatectomy. N Engl J Med 2002;346:1138-44.
23. Shen T, Weissleder R, Papisov M, Bogdanov A, Brady T. Monocrystalline iron oxide nanocompounds (MION): physiochemical properties. Magn Reson Med 1993;29:599-604.
24. Jager GJ, Barentsz JO, Oosterhof GO, Witjes JA, Ruijs SJ. Pelvic adenopathy in prostatic and urinary bladder carcinoma: MR imaging with a three-dimensional T1-weighted magnetization-prepared-rapid gradient-echo sequence. AJR Am J Roentgenol 1996;167:1503-7.
25. Metz CE. ROC methodology in radiologic imaging. Invest Radiol 1986;21:720-33.
26. Landis JR, Koch GG. The measurement of observer agreement for categorical data. Biometrics 1977;33:159-74.
27. Partin AW, Kattan MW, Subong EN, et al. Combination of prostate-specific antigen, clinical stage, and Gleason score to predict pathological stage of localized prostate cancer: a multi-institutional update. JAMA 1997;277:1445-51. [Erratum, JAMA 1997;278:118.]
28. Beissner RS, Stricker JB, Speights VO, Coffield KS, Spiekerman AM, Riggs M. Frozen section diagnosis of metastatic prostate adenocarcinoma in pelvic lymphadenectomy compared with nomogram prediction of metastasis. Urology 2002;59:721-5.
29. Bolla M, Gonzalez D, Warde P, et al. Improved survival in patients with locally advanced prostate cancer treated with radiotherapy and goserelin. N Engl J Med 1997;337:295-300.
30. Anzai Y, Blackwell KE, Hirschowitz SL, et al. Initial clinical experience with dextran-coated superparamagnetic iron oxide for detection of lymph node metastases in patients with head and neck cancer. Radiology 1994;192:709-15.
31. Stets C, Brandt S, Wallis F, Buchmann J, Gilbert FJ, Heywang-Kobrunner SH. Axillary lymph node metastases: a statistical analysis of various parameters in MRI with USPIO. J Magn Reson Imaging 2002;16:60-8.
32. Pannu HK, Wang KP, Borman TL, Bluemke DA. MR imaging of mediastinal lymph nodes: evaluation using a superparamagnetic contrast agent. J Magn Reson Imaging 2000;12:899-904.
33. Michel SC, Keller TM, Frohlich JM, et al. Preoperative breast cancer staging: MR imaging of the axilla with ultrasmall superparamagnetic iron oxide enhancement. Radiology 2002;225:527-36.
34. de Jong IJ, Pruim J, Elsinga PH, Vaalburg W, Mensink HJ. Visualization of prostate cancer with 11C-choline postiron emission tomography. Eur Urol 2002;42:18-23.
35. Campbell SC, Klein EA, Levin HS, Piedmonte MR. Open pelvic lymph node dissection for prostate cancer: a reassessment. Urology 1995;46:352-5.